CFD-DEM Simulation of Turbulence Modulation in Horizontal Pneumatic Conveying

CFD-DEM Simulation of Turbulence Modulation in Horizontal Pneumatic Conveying

Mohammadreza Ebrahimi[1], Martin Crapper[2]

[1]*Institute for Infrastructure and Environment, School of Engineering, the University of Edinburgh, Edinburgh EH9 3JL, UK*

[2]*Department of Mechanical and Construction Engineering, Northumbria University, Ellison Place, Newcastle-upon-Tyne, NE1 8ST, UK*

Abstract

A study is presented to evaluate the capabilities of the standard k-ε turbulence model and the k-ε turbulence model with added source terms in predicting the experimentally measured turbulence modulation due to the presence of particles in horizontal pneumatic conveying, in the context of a CFD-DEM Eulerian-Langrangian simulation. Experiments were performed using a 6.5 m long, 0.075 m diameter horizontal pipe in conjunction with a laser Doppler anemometry (LDA) system. Spherical glass beads with two different sizes, 1.5 mm and 2 mm, were used. Simulations were carried out using the commercial Discrete Element Method (DEM) software EDEM, coupled with the Computational Fluid Dynamics (CFD) package FLUENT. Hybrid source terms were added to the conventional k-ε turbulence model to take into account the influence of the dispersed phase on the carrier phase turbulence intensity. The simulation results showed that the turbulence modulation depends strongly on the model parameter $C_{\varepsilon 3}$. Both the standard k-ε turbulence model and the k-ε turbulence model with the hybrid source terms could predict the gas phase turbulence intensity trend only generally, with in all cases a noticeable discrepancy between simulation and experimental results was observed, particularly for the regions close to the pipe wall. It was also observed that in some cases the addition of the source terms to the k-ε turbulence model did not improve the simulation results when compared to the simulation results of the standard k-ε turbulence model, though in the lower part of the pipe where particle loading was greater due to gravitational effects the model with added source terms performed somewhat better.

Keywords: Turbulence modulation, Pneumatic conveying, Eulerian-Lagrangian approach, Laser Doppler anemometry

1. INTRODUCTION AND BACKGROUND

1.1. Turbulence Modulation in Fluid-Particle Flows

Carrier phase turbulence structure changes as a particulate phase is added to a clear fluid phase. This phenomenon is referred to as turbulence modulation in the literature (Elgobashi & Abou-Arab, 1983). It is important because any change in continuous phase turbulence has a direct influence on the fluid mean velocity, heat and mass transfer as well as particle mixing and dispersion (Fokeer, Kingman, Lowndes, & Reynolds, 2004; Kenning & Crowe, 1997; Lightstone & Hodgson, 2004). It has also been pointed out that in a dilute phase particle laden flow, turbulence modulation impacts drastically on the conveying line pressure drop (Curtis & van Wachem, 2004). Laín, Bröder, Sommerfeld, and Göz (2002) also highlighted the influence of turbulence modulation on the prediction of the hydrodynamic behaviour of a bubble in a bubble column. Therefore it seems that understanding the interaction between a dispersed phase and fluid phase turbulence is one of the crucial steps in understanding the complex characteristics of two-phase systems.

Both attenuation and augmentation of fluid phase turbulence have been reported in previous studies. Despite much research focused on this topic, there is no generally accepted explanation for the influence of the solid phase on the carrier phase (Crowe, 2000; Mandø, 2009). In general, it is recognizable from previous studies that small particles tend to suppress the carrier phase turbulence level while large particles increase it. Previous observations reveal that small particles (particle diameter $d_p < 200$ μm) follow the fluid flow and as a result these particles may break turbulent eddies. These small particles may be accelerated by eddies, and so extract kinetic energy from them (dissipation of energy), leading to a reduction in the turbulence level of the fluid flow (Geiss, et al., 2004; Lightstone & Hodgson, 2004). On the other hand, fluid flow turbulence augmentation by large particles can be explained as a result of the wake generated behind the particles. This wake creates an additional disturbance to the flow which may increase the level of turbulence. These phenomena are considered to be the core reasons of turbulence reduction and enhancement (Bolio & Sinclair, 1995).

In addition to these two predominant mechanisms, other factors such as fluid flow turbulence modification due to particle-particle interaction, changes in turbulence dissipation as a result of the introduction of new length scales and changes in the continuous phase velocity gradient are believed to be other influential reasons for turbulence modification. However, these

mechanisms may be negligible in a dilute particle suspension (Yuan & Michaelides, 1992). Lightstone and Hodgson (2004) also mentioned the influence of the crossing trajectory, i.e. the relative mean velocity between the particles and the turbulence eddies, as another source of gas phase turbulence generation.

Some researchers have tried to formulate turbulence modulation based on the observation of experimental results (Crowe, 2000; Mandø, 2009). However these formulations are valid only for the specific range of solid loading ratios and system specifications observed in each case.

According to the explanation regarding the turbulence modulation, it seems that particle size, particle concentration (loading), fluid velocity and ratio of particle to fluid length scale are important parameters to evaluate the turbulence modulation. These four parameters may be expressed as 1) mass /volumetric solid loading, 2) the ratio of particle diameter to the fluid turbulence length scale 3) particle Reynolds number ($Re_p = \rho(v - u_p)d_p/\mu$) and 4) Stokes number ($St = \tau_p/\tau_e$) (Fokeer, et al., 2004; Gouesbet & Berlemont, 1998; Mandø, 2009; Yarin & Hetsroni, 1994) where ρ is the fluid density, v is the fluid velocity, u_p is the particle velocity, d_p is particle diameter and μ is the dynamic viscosity. τ_p and τ_e are particle response time and eddy turnover time respectively.

Based on the Elghobashi (1994) study, for particle volume fraction less than 10^{-6}, the influence of particles on the fluid phase turbulence is weak. For particle volume fractions in the range $10^{-6} < \phi_p < 10^{-3}$, the particles can augment or attenuate the carrier phase turbulence depending on the ratio of τ_p/τ_e. For $\tau_p/\tau_e < 1$, the turbulence is reduced by the particle presence while for $\tau_p/\tau_e > 1$ the carrier phase turbulence is enhanced. Elghobashi (1994) also explained turbulence augmentation due to the wake formation.

Gore and Crowe (1989) reviewed the wide range of experimental data for pipe and jet flows and suggested that the ratio of particle diameter (d_p) to the integral length scale (l_e) may be used as a criterion to examine the augmentation or attenuation of turbulence level. The length scale ratio 0.1 is a distinguishing point for turbulence modulation; for a length scale ratio $d_p/l_e < 0.1$ turbulence intensity decreases while for $d_p/l_e > 0.1$, particles tend to increase the turbulence intensity.

Hetsroni (1989) investigated various experimental data for horizontal and vertical two-phase pipe flows and concluded that particles with Re_p higher than 400 tend to increase the turbulence intensity due to vortex shedding from particles, while particles with Re_p less than 400 tend to suppress the turbulence intensity. Yuan and Michaelides (1992) also noted that a wake behind a particle is formed for $Re_p > 20$ and for $Re_p > 400$ vortices are shed behind the solid particles. Lun (2000) also reported that turbulence modulation depends significantly on Re_p; however he found vortex shedding occurs when Re_p is around 300. He observed that particles tend to attenuate the carrier phase turbulence when $Re_p < 300$, whilst on the other hand if the Re_p is more than a critical Re_p, turbulence enhances.

1.2. Previous Experimental Work on Turbulence Modulation

As laser Doppler anemometry (LDA) is a non-contact optical measurement which can handle velocity components with high temporal and spatial resolution, it has been used extensively for measuring gas and particle velocities in gas-solid flows (Fan, Zhang, Cheng, & Cen, 1997; Y. Lu, Glass, Easson, & Crapper, 2008; Y. Lu, Glass, & Easson, 2009; Mathisen, Halvorsen, & Melaaen, 2008; Tsuji & Morikawa, 1982). Tsuji and Morikawa (1982) observed that air flow turbulence level depended heavily on particle size, that 3.4 mm particles increased the turbulence while 0.2 mm particles reduced it. The influence of the particle size on the carrier phase turbulence level also reported by (Tsuji, Morikawa, & Shimoni, 1984) and (Henthorn, Park, & Curtis, 2005). Fan, et al. (1997) applied laser Doppler anemometry (LDA) to measure both phases' velocity and turbulence intensity in dilute vertical pneumatic conveying and compared experimental measurements with simulation. They concluded that the turbulence intensity of the gas phase was attenuated and the mean gas velocity profile was flattened by adding particles. Turbulence intensity reduction by adding fine particles (50-90 μm) was also mentioned by Kulick, Fessler, and Eaton (1994) observing that the degree of attenuation increased by increasing the particle mass loading ratio and distance from the wall.

1.3. Numerical Modelling of Turbulence Modulation

Generally, to model the turbulence modulation phenomenon, source terms are added to the single phase flow equations for turbulent kinetic energy and dissipation to take into account the presence of the solid phase. Some research has been conducted to formulate these source terms (Geiss, et al., 2004; Gouesbet & Berlemont, 1998; Rao, Curtis, Hancock, & Wassgren, 2012). These formulations mainly depend on the turbulence model used to close the fluid

momentum equation (Laín & Sommerfeld, 2003). Since the k–ε is the most common turbulence model in single phase flow modelling, consequently most of the source terms are derived for turbulent kinetic energy and dissipation equations of this model (Chen & Wood, 1985; Fan, et al., 1997; Pakhomov, Protasov, Terekhov, & Varaksin, 2007). However, source terms for other turbulence models like Reynolds stress turbulence model and k-ω have also been derived (Laín & Sommerfeld, 2008; Lun, 2000). These source terms can be divided into three main methods based on the original equations that these source terms have been derived from (Boulet & Moissette, 2002; Laín, et al., 2002; Mandø, 2009). These are standard, consistent and hybrid methods. In fact, the hybrid method is the combination of standard and consistent methods (Mandø, 2009). Here, these categories are explained for k-ε turbulence model.

1.3.1. Standard and Consistent Approaches

The general form of the source term due to the dispersed phase in the turbulent kinetic energy equation for the standard method may be expressed as equation (1) (Chen & Wood, 1985; Gouesbet & Berlemont, 1998):

$$S_{kp} = \overline{S'_{pv_i} v'_i} \tag{1}$$

where S_{kp} is the source term in the turbulent kinetic energy equation and S'_{pv_i} is the source term in fluctuating momentum exchange term. If we assume that the interaction between the two phases occurs only due to the drag force, then equation (1) can be written as

$$S_{kp} = \frac{\phi_p \rho_p}{\tau_p(C_D)} (\overline{u'_{pi} v'_i} - \overline{v'_i v'_i}) \tag{2}$$

where ϕ_p, ρ_p and C_D represent the particle volume fraction, particle density and drag coefficient respectively. v'_i is gas fluctuating velocity and u'_{pi} is particle fluctuating velocity. $\overline{v'_i v'_i}$ is modelled as for the clear gas phase as used in the standard k–ε model, which is $\overline{v'_i v'_i} = 2k$. However $\overline{u'_{pi} v'_i}$ still requires to be modelled (Lightstone & Hodgson, 2004). Some models have been presented in Lightstone and Hodgson (2004) for the k–ε model. As stated by Boulet and Moissette (2002), u'_{pi} arises from particle-particle and particle-wall interaction, and is often smaller than v'_i resulting in S_{kp} being negative. Therefore, this approach can only predict the dissipation of the carrier phase turbulence (Boulet & Moissette, 2002; Laín, et al., 2002;

Mandø, 2009). One may conclude that this method is not suitable for the modelling of turbulence modulation due to large particles which enhance turbulence intensity.

The consistent method derives from Crowe (2000). It starts with the mechanical energy equation for the fluid phase. The source term in the turbulent kinetic energy equation considering the drag force as the only interaction force is expressed as:

$$S_{kp} = \frac{\phi_p \rho_p}{\tau_p(C_D)} \left(\left| \overline{v_i} - \overline{u_{pi}} \right|^2 + \left(\overline{u'_{pi} u'_{pi}} - \overline{v'_i u'_{pi}} \right) \right) \tag{3}$$

The first contribution may be explained as the kinetic energy production due to the particle drag. In fact, this term takes into account turbulence generation due to the particle wake. The second term (redistribution) is attributed to the transfer of the kinetic energy of the particle motion into the kinetic energy of the continuous phase. This second term has a negligible effect in dilute suspensions. Hwanc and Shen (1993) also presented the same formulation, however they did not limit the momentum exchange term to the drag force.

Since larger and heavier particles are conveyed with lower velocity, the first term in equation (3) has a higher value when compared to the conveying of smaller particles which are conveyed with higher velocity. Generally, the generation due to the particle drag has a larger magnitude than the redistribution term. As a result one may notice that models based on this approach are capable of capturing fluid phase turbulence augmentation only, and may not be suitable to be applied for turbulence modulation due to small particles.

1.3.2. Hybrid Method

With regard to the limitations of the previous methods of simulating turbulence modulation, the hybrid method was suggested by (Geiss, et al., 2004). The hybrid source term for the k–ε model can be seen in equation (4). Only the drag force was considered as a gas-solid interaction force and the influence of particle-particle collisions on the turbulence modulation was neglected.

$$S_{kp} = \frac{\phi_p \rho_p}{\tau_p(C_D)} \left(\left| \overline{v_i} - \overline{u_{pi}} \right|^2 + \left(\overline{u'_{pi} u'_{pi}} - \overline{v'_i v'_i} \right) \right) \tag{4}$$

This source term can also be derived by adding the standard and consistent method source terms (Mandø, 2009). As mentioned for the consistent approach, the first term represents the

conversion of mechanical energy by the drag force into turbulent kinetic energy. The particle fluctuating velocity in the second term is important only in the case of dense flows or for the regions close to the wall. As a result, in dilute suspensions, this term can be omitted for simplicity (Geiss, et al., 2004). Again, $\overline{v_i' v_i'}$ can be replaced by $2k$, meaning that equation (4) can be written as

$$S_{kp} = \frac{\Phi_p \rho_p}{\tau_p (C_D)} \left(\left| \overline{v_i} - \overline{u_{pi}} \right|^2 - 2k \right) \tag{5}$$

This formulation can predict both the increase and decrease of carrier phase turbulence intensity. For small particles travelling at almost the same velocity as the carrier phase, the effect of the first term is negligible and overall the source term decreases the turbulence intensity. For large particles, on the other hand, the first contribution is significantly bigger than the second term leading to turbulence augmentation.

Mandø (2009) also derived the same equation as equation (4) by using the Vreman (2007) study. He showed the ability of this model by implementing it in an Eulerian-Eulerian framework and evaluated its ability against several experimental results for dilute vertical gas-particle flows for a various range of solid loading ratios (SLR= solid mass flow rate/ gas mass flow rate), particle sizes and Re_p. A good agreement between the turbulence intensity measured experimentally and calculated by the model was observed.

For all approaches mentioned above, the dissipation term due to the presence of particles, $S_{\varepsilon p}$, is assumed to be proportional to S_{kp} and the ratio $\frac{\varepsilon}{k}$ (Laín, et al., 2002):

$$S_{\varepsilon p} = C_{\varepsilon 3} \frac{\varepsilon}{k} S_{kp} \tag{6}$$

The empirical constant $C_{\varepsilon 3}$ does not have a unique value and various values have been proposed ranging from 1.0 to 2.0 (Zhang & Reese, 2003). Boulet and Moissette (2002) reported that $C_{\varepsilon 3}$ depends mainly on particle concentration and diameter and it is not a universal constant. They also mentioned that the method of derivation of S_{kp} leads to a different value for $C_{\varepsilon 3}$. Geiss, et al. (2004) applied the value of 1.87 for $C_{\varepsilon 3}$ while Mandø (2009) obtained good results by setting the constant to 1.00. Laín, et al. (2002) used a value of 1.8 in the simulation of a bubble column. Boulet and Moissette (2002) applied 1.8 for modelling a vertical gas-particle flow; they showed the fluid phase turbulence value depended strongly on the value of $C_{\varepsilon 3}$. They also showed a

small change in the $C_{\varepsilon 3}$ value (from 1.8 to 1.85 or 1.8 to 1.81) could change the simulation results considerably. They concluded that the value of $C_{\varepsilon 3}$ which gives the best result for one example may not be suitable for another example if there is a change in the volume fraction.

Zhang and Reese (2003) reported that, for large and heavy particles with the ratio of the particle relaxation time to time scale of the large eddies around 10, $C_{\varepsilon 3}$ was decreased by increasing the mass loading. They proposed to replace the $C_{\varepsilon 3}$ in equation (6) with $C_{\varepsilon 3,c}$ based on equation (7), which is dependent on the particle volume fraction:

$$C_{\varepsilon 3,c} = \left[1 - \left(\frac{6\phi_p}{\pi\phi_{p,m}}\right)^{1/3}\right] C_{\varepsilon 3} \qquad (7)$$

where $\phi_{p,m}$ is the random close-packing particle volume fraction, which is assumed to be 0.64. As can be seen from equation (7), $C_{\varepsilon 3,c}$ depends on the initial selection of $C_{\varepsilon 3}$ .They selected the value of 1.95 for $C_{\varepsilon 3}$ which best matches Tsuji and Morikawa (1982)'s experimental results, and also showed that the predicted turbulent kinetic energy depended significantly on the value of $C_{\varepsilon 3}$.

In summary the number of studies covering the simulation of turbulence modulation in particle laden flow is very limited and our study is intended to begin addressing this situation.

1.4. Aims

The aim of our study is to evaluate the capabilities of the standard k-ε turbulence model and the k-ε turbulence model with added source terms in predicting the experimentally measured turbulence modulation in horizontal pneumatic conveying in the context of a CFD-DEM Eulerian-Langrangian simulation. To achieve this goal, a series of experiments was conducted to measure the turbulence level of the gas phase in the presence of particles using the LDA technique in a horizontal pneumatic conveying line. The hybrid source terms were added to the conventional k-ε turbulence model in the FLUENT-EDEM, CFD-DEM framework via User-Defined Functions (UDF) and the simulation results were compared with the experimental data.

2. EXPERIMENTS

Figure 1 displays the schematic sketch of the horizontal pneumatic conveying experiment. The y negative direction is in the gravity direction, the z positive axis is along the pipe and the x positive direction is outward from the page. The pneumatic conveying system consists of a hopper, fan, cyclone and conveying line. The particles are pushed by a screw feeder into the inclined pipe (inclined at 45°) which is connected to the horizontal pipe. Once inside the horizontal pipe, the fan sucks both the gas (air) and the particles into the cyclone at the downstream end, where they are separated. The horizontal section is 6.5 m long and is connected to the vertical section (1.2 m) by a bend. The pipe internal diameter is 0.075 m. Measurements were carried out for a cross section at distance of 2 m from the point where the particles are introduced to the horizontal section (shown by the red arrow). This cross section is called z=2 m. The particle flow rate can be regulated by adjusting the screw feeder speed and air flow rate can also be regulated; this makes it possible to obtain the desired SLRs in the conveying line. Two different glass bead particles (spherical, diameters of 2 mm and 1.5 mm, 2540 kg/m^3 density) were used in the experiments. Two different SLRs were produced by combining the two different mean gas velocities (9.5 and 8.5 m/s) with fine adjustment of the screw feeder speed. Particle flow rates were set to 0.1128 kg/s and 0.1329 kg/s. The resulting SLRs were 2.3 and 3.

The LDA technique is used to measure the axial mean gas velocity and axial fluctuating root mean square velocity (v'_{rms}) . The laser beams are refracted while passing through the pipe's curved wall. As a result, there would be a deviation between the actual beam intersection point and the expected position, so in order to find the intersection point accurately inside the pipe the method suggested by Y. Lu, et al. (2009) was adopted .

The first velocity measurement was at the pipe centre, and then the probes were moved horizontally and vertically to measure the mean gas velocity and v'_{rms} for other measurement points across the pipe. The distance between every two measurement points is 5 mm. In total, twenty six velocity measurements were performed for the pipe cross section, including thirteen measurements in the horizontal direction and thirteen measurements in the vertical direction. The measurement reproducibility was checked by repeating the measurements three times, and each measurement was carried out for 50 seconds. For the present study, the size difference

between the tracer particles (incense smoke) and the glass beads is considerable, ensuring that only one velocity (carrier phase or solid phase) was measured at any given time.

The axial mean velocity for gas at a sample point (x, y, z) is calculated according to equation (8):

$$\overline{v} = \frac{1}{N}\sum_{i=1}^{N} v_i \tag{8}$$

where v_i is the axial instantaneous gas velocity component and $\bar{v}$ is the axial mean gas velocity. N is the number of samples at the measurement point. The gas fluctuating root mean square velocity is calculated using the following equation:

$$v'_{rms} = \sqrt{\frac{1}{N}\sum_{i=1}^{N}(v_i - \overline{v})^2} \tag{9}$$

These data from LDA measurements are used to calculate turbulence intensity:

$$\sigma = v'_{rms}/\overline{v} \tag{10}$$

3. SIMULATION

Simulation was carried out using the commercial software Ansys FLUENT version 12.1 and EDEM version 2.4 in an Eulerian-Lagrangian framework, in which particles are tracked individually. The locally averaged Navier-Stokes equations in connection with the standard k-ε are solved in FLUENT and the hybrid source terms are added to the standard k-ε model via User-Defined Functions (UDF). The motion of discrete phase is described by solving Newton's laws of motion. The two softwares are coupled with full momentum and volume fraction exchange between the solid and fluid phases (two-way coupling). The governing equations for gas flow are conservation of mass and momentum:

$$\frac{\partial\left(1-\phi_p\right)\rho}{\partial t} + \nabla.\left(1-\phi_p\right)\rho\bar{v} = 0 \tag{11}$$

$$\begin{aligned}\frac{\partial(1-\phi_p)\rho\bar{v}}{\partial t} &+ \nabla.\left(1-\phi_p\right)\rho\bar{v}\bar{v} \\ &= -\nabla \mathrm{p} + \nabla.\left(\left(1-\phi_p\right)\tau\right) + \nabla.\left(\left(1-\phi_p\right)\tau'\right) \\ &+ (1-\phi_p)\rho g - S\end{aligned} \tag{12}$$

$$S = \frac{\sum_i^n F_{interaction,i}}{\Delta V} \tag{13}$$

τ is the fluid viscous stress tensor, τ' is the Reynolds stress tensor, S is the volumetric force acting on each mesh cell and $F_{interaction,i}$ includes drag and lift forces. n and ΔV are the number of particles in the considered computational cell and the computational cell volume respectively. Drag force was simulated by the Ergun (1952) and Wen and Yu (1966) model. In our previous study Ebrahimi, Crapper, and Ooi (2014) it was found that, the inclusion of Magnus lift force due to particle rotation was essential to reproduce the general behaviour observed in the experiments. Therefore, the Magnus lift force equation based on the Oesterlé and Dinh (1998) research was implemented in the all simulations. The general *k-ε* turbulence model equations in FLUENT are expressed as follow:

$$\frac{\partial}{\partial t}(\rho k) + \frac{\partial}{\partial x_i}(\rho k v_i) = \frac{\partial}{\partial x_i}\left[\left(\mu + \frac{\mu_t}{\sigma_k}\right)\frac{\partial k}{\partial x_i}\right] + G_k + G_b - \rho\varepsilon - Y_M + S_{kp} \tag{14}$$

$$\frac{\partial}{\partial t}(\rho \varepsilon) + \frac{\partial}{\partial x_i}(\rho \varepsilon v_i v_i) = \frac{\partial}{\partial x_i}\left[\left(\mu + \frac{\mu_t}{\sigma_\varepsilon}\right)\frac{\partial \varepsilon}{\partial x_i}\right] + C_{\varepsilon 1}\frac{\varepsilon}{k}(G_k + C_{\varepsilon 3}G_b) - C_{\varepsilon 2}\rho\frac{\varepsilon^2}{k} + S_{\varepsilon p} \tag{15}$$

$\mu_t = \rho C_\mu \frac{k^2}{\varepsilon}$ is the turbulent eddy viscosity , σ_k and σ_ε are turbulence Prandtl numbers and S_{kp} and $S_{\varepsilon p}$ are replaced by the model suggested by Geiss, et al. (2004) and Mandø (2009) (hybrid source terms equations (5) and (6)). Translational and rotational motions of particles are determined by the equations below.

$$m_i \frac{du_{p,i}}{dt} = m_i g + \sum_{j=1}^{n} F_{contact\ i,j} + \sum_{i=1}^{n} F_{interaction,i} \tag{16}$$

$$I_i \frac{d\omega_{p,i}}{dt} = \sum_{j=1}^{n} T_{i,j} \tag{17}$$

where m_i is the mass of particle i, $u_{p,i}$ is the particle i velocity, $F_{contact\ i,j}$ is the contact force of particle i and particle j or wall and $F_{interaction,i}$ shows the particle-fluid interaction. $\omega_{p,i}$ and I_i are the angular velocity and moment of inertia of particle i, respectively and $T_{i,j}$ is the torque of particle i that interacts with particle j or wall. A non-linear Hertz-Mindlin contact model was applied in the simulation. Normal force and normal damping force are given by:

$$F_n = \frac{4}{3} Y^* \delta_n^{3/2} \sqrt{R^*} \tag{18}$$

$$F_n^d = -2\sqrt{5/6}\,\beta\sqrt{S_n m^*} V_n^{rel} \tag{19}$$

$$S_n = 2Y^*\sqrt{R^*\delta_n} \tag{20}$$

$$\beta = \frac{\ln e}{\sqrt{\ln^2 e + \pi^2}} \tag{21}$$

where Y^*, δ_n , m^*, R^*, e are the equivalent Young's modulus, the normal overlap, the equivalent mass, the equivalent radius and coefficient of restitution respectively. Tangential force and damping are calculated by the following equations (Mindlin & Deresiewicz, 1953)

$$F_t = -S_t \delta_t \tag{22}$$

$$S_t = 8G^*\sqrt{R^*\delta_n} \tag{23}$$

$$F_t^d = -2\sqrt{5/6}\,\beta\sqrt{S_t m^*} V_t^{rel} \tag{24}$$

where δ_t is the tangential overlap and $G^*$is the equivalent shear modulus. The tangential force is limited by the Coulomb friction ($\mu_s F_n$) where μ_s represents the static friction coefficient. If the net tangential force reaches the frictional force then sliding occurs. The rolling friction is accounted for by applying a torque to the contacting surfaces which is a function of normal force F_n and coefficient of rolling friction μ_r.

$$\tau_{r,i} = -\mu_r F_n R_i \omega_i \tag{25}$$

A three-dimensional mesh was built to simulate the experimental apparatus. Due to the requirements of the CFD-DEM coupling, a fluid mesh size which was three to five times bigger than the particle size was selected. However, it is one of the limitations in the coupled CFD-DEM that the mesh size cannot be resolved finely and as a result the fluid detail may not be captured accurately. The domain was divided into 205,490 tetrahedral mesh elements, with 397,376 nodes. To decrease the computational time, only 2.2 m of horizontal pipe was simulated. The gas velocity profile at 2.2 m along the pipe was measured by the aid of LDA

and this experimentally measured velocity profile then was used as a boundary condition in the simulation. Particles in the simulations are created in the inclined pipe attached to the horizontal pipe, with an initial velocity of 0.0635 m/s in the x direction. This initial velocity is given to the particles to replicate the screw feeder effect, since the screw feeder is not modelled explicitly. The particles roll down the inclined pipe surface and are pulled down by the effect of gravity into the horizontal pipe where they experience a gas flow similar to the experiments. All parameters used in the pneumatic conveying simulation in FLUENT-EDEM are summarized in Table 1.

4. RESULTS AND DISCUSSION

4.1. Simulation of Turbulence Intensity in Single Phase Flow

Firstly, the simulation results for single-phase turbulence intensity are compared with the experimental measurements. As seen in Figure 2 and Figure 3, the simulations give good agreement with the single phase experimental measurements.

4.2. Effect of the Constant $C_{\varepsilon 3}$ on Turbulence Modulation in Particle Laden Flow

To determine whether or not the $C_{\varepsilon 3}$ value had a significant effect on the simulation results, four different values for $C_{\varepsilon 3}$, all reported in the literature, were selected. Simulation results for horizontal profile of turbulence intensity at z=2 m for SLR=2.3 and SLR=3 in the presence of 2 mm glass beads are shown in Figure 4 and Figure 5. It is seen that the turbulence intensity values depend strongly on the $C_{\varepsilon 3}$. For both cases, by increasing the $C_{\varepsilon 3}$ values from 1.1 to 1.89, turbulence intensity drops noticeably. This is in a good agreement with the Zhang and Reese (2003) study which reported that the $C_{\varepsilon 3}$ values had a significant effect on fluctuating gas velocity. It is also seen that for regions close to the wall, turbulence intensity increases significantly.

Figure 6 shows the vertical profile of turbulence intensity of air in the presence of 2 mm glass beads at z=2 m for SLR=2.3. These results also indicate that the turbulence intensity values change considerably by changing $C_{\varepsilon 3}$. It is also seen that the higher the $C_{\varepsilon 3}$ value, the lower the turbulence intensity. Moreover, it is seen that the turbulence intensity value is not symmetric; it is higher in the lower section of the pipe because the number of particles here is higher and

lower in the pipe upper section where the particle concentration is much lower. This trend was previously observed experimentally by (Tsuji & Morikawa, 1982).

If the simulation results presented in Figure 4 and Figure 5 are summarized in one graph, the influence of SLR on the turbulence intensity for a constant $C_{\varepsilon 3}$ can be seen (Figure 7). For instance, if turbulence intensity for SLR=2.3, $C_{\varepsilon 3}$=1.7 is compared with SLR=3, $C_{\varepsilon 3}$=1.7, it becomes clear that the simulated turbulent intensity increases with increasing SLR. The same trend is seen when SLR=2.3, $C_{\varepsilon 3}$=1.8 is compared with SLR=3, $C_{\varepsilon 3}$=1.8. It shows that the turbulence intensity increases by increasing the SLR for a constant $C_{\varepsilon 3}$ as was previously reported in Curtis & van Wachem, 2004.

The results from Figure 4 to Figure 7 confirm that the new source terms added to the k-ε turbulence model are capable of predicting previously reported trends.

4.3. Comparison with Experimental Results

In order to evaluate the influence of the source terms added to the standard k-ε turbulence model, simulation results were compared with experimental results. The results for horizontal and vertical profiles of carrier phase turbulence intensity in the presence of 1.5 mm glass beads with SLR=3 are shown in Figure 8 and Figure 9 respectively. It is seen that turbulence intensity decreases with increasing the $C_{\varepsilon 3}$. In the horizontal profile, the k-ε model with the source terms and $C_{\varepsilon 3}$=1.8 is under-predicting the experimental results considerably due to the overestimation of the dissipation. Obviously, the turbulence intensity predicted by the k-ε turbulence model with the source terms with $C_{\varepsilon 3}$=1.1 is over-predicting the turbulence intensity compared to the experimental results in the central section of the pipe.

In the central regions of the pipe, the standard k-ε turbulence model without the source terms can predict the experimental results more accurately when compared to the simulation results with the k-ε turbulence model with the source terms. However, in the regions closer to the pipe walls, the simulation results with the k-ε turbulence model with the source terms and $C_{\varepsilon 3}$=1.5 or 1.7 are closer to the experimental data when compared with the simulation results obtained by the standard k-ε turbulence model. The experimental turbulence intensity trend is captured

only very generally by the turbulence models in the horizontal profile, and the model shows significant turbulence intensity increase only for regions very close to the pipe wall.

As is seen, the experimentally measured turbulence intensity data is non-symmetric along the horizontal profile. This can be explained by the fact that the particles enter at one side of the inclined pipe, which is then connected to the horizontal pipe (please refer to Figure 1), so it can be expected that there is a different particle number in x direction, and as a result non-symmetric experimental data was measured.

In the vertical profile, the simulation results obtained from the standard k-ε turbulence model are closer to the experimental data in the central region of pipe compared to the simulation results obtained from the k-ε turbulence model with source terms. However, since there is no term in the standard k-ε turbulence model to take into account the presence of particles, the increase in turbulence intensity in the lower region of pipe where more particles are concentrated due to gravity cannot be modelled accurately. Similar to the experimental measurements, the k-ε turbulence model with the source terms and $C_{\varepsilon 3}$=1.1, 1.5 or 1.7 predicts higher turbulence intensity values in the lower half of the pipe which are relatively close to the experimental data. Lower turbulence intensity values in the pipe upper section where fewer particles are transported are obtained when compared to the turbulence intensity values in the pipe lower section by turbulence model with or without source terms. For both horizontal and vertical profiles, the discrepancy between experimental and simulation results increases toward the walls as previously observed by Boulet and Moissette (2002) in vertical pneumatic transportation.

The capacity of the CFD-DEM approach to simulate the near-wall flow is generally limited, as the fluid mesh cannot be resolved finely enough for this due to the requirement for it to be significantly larger than the particle diameter. Moreover, in the implemented hybrid source terms, the effect of the particle fluctuating velocity i.e. $\overline{u'_{pi}u'_{pi}}$ was omitted for model simplicity. However, for near-wall regions it can be imagined that the gas phase turbulence intensity will be altered due to the significant increase of particle fluctuating velocity due to the increased particle-wall collisions.

Simulation and experimental results of carrier phase turbulence intensity in the presence of 1.5 mm glass beads, SLR=2.3 are shown in Figure 10 and Figure 11. In the horizontal profile and close to the pipe centre, a close agreement between the experimental data and the simulation results obtained by the standard k-ε turbulence model is observed. The k-ε turbulence model with the source terms over-estimates the turbulence intensity except for $C_{\varepsilon 3}$=1.8. Similar to Figure 8, the model is not capable of capturing the detail of the experimental results. In the vertical profile, the significant increase in the turbulent intensity in the lower section of pipe is not captured by the standard k-ε turbulence model. In this case, the simulations with $C_{\varepsilon 3}$=1.7 or $C_{\varepsilon 3}$=1.1 are closest to the experimental results. The turbulence intensity trend is captured generally by the k-ε turbulence model with the source terms.

Comparison between experimental and simulation results of horizontal and vertical profiles of gas phase turbulence intensity in the presence of 2 mm glass beads for SLR=2.3 are presented in Figure 12 and Figure 13. As can be seen, the simulation results with $C_{\varepsilon 3}$=1.8 or $C_{\varepsilon 3}$=1.7 are close to the experimental results in the central section of the pipe in both horizontal and vertical profiles. However, the discrepancy increases for the measurement points closer to the pipe walls. Similar to the previous simulations, the turbulence intensity increases in the lower half of the pipe is not captured by the standard k-ε turbulence model (Figure 13).

Figure 14 and Figure 15 show the carrier phase turbulence intensity for the particle laden flow with 2 mm glass beads, SLR=3. As is seen, the simulation results obtained from the standard k-ε turbulence model and the k-ε turbulence model with $C_{\varepsilon 3}$=1.8 are similar. A very good agreement between the simulation with $C_{\varepsilon 3}$=1.8, the standard k-ε turbulence model and experimental results in the horizontal profile is observed, except for the measurement points close to the pipe walls. In the vertical profile, a good agreement is also observed between the experimental results and simulation results with $C_{\varepsilon 3}$=1.8 in the central parts of the pipe (Figure 15).

From all comparisons between experimental and simulations results presented in this section, it was observed that neither the k-ε turbulence model with hybrid source terms nor the standard k-ε turbulence model could predict accurately the carrier phase turbulence intensity in a horizontal pneumatic conveying experiment using a CFD-DEM approach. However, the

general behaviour was captured. It was found that in some cases the addition of source terms could not improve the simulation results.

It also was observed that the turbulence model is very sensitive to the $C_{\varepsilon 3}$ values. Therefore, if source terms are used, this value needs to be calibrated before every simulation depending on the particle size and SLR. In the current study it was observed that as $C_{\varepsilon 3}$ reached 1.7 or 1.8 a further increase of $C_{\varepsilon 3}$ values changed the simulation results significantly. However, more simulations with various operating conditions (i.e. different SLRs) are required to be performed before any conclusion can be made regarding the critical $C_{\varepsilon 3}$ values.

5. CONCLUSIONS

The turbulence modulation phenomenon was investigated experimentally and numerically. The LDA technique was used to measure turbulence intensity in a horizontal pneumatic conveying line in the presence of 1.5 and 2 mm spherical glass beads for two SLRs, 2.3 and 3. Simulations were carried out in an Eulerian-Lagrangian framework using the commercially CFD-DEM coupled code FLUENT-EDEM. User-defined functions were used to add hybrid source terms to the standard k-ε turbulence model to simulate turbulence modulation due to particles. Simulation results revealed that the simulated turbulence intensity depends on the value of the constant $C_{\varepsilon 3}$ and the higher the $C_{\varepsilon 3}$, the lower the turbulence intensity. It was also shown that the higher the SLR, the higher the turbulence intensity. In vertical profiles, simulation results predicted the higher turbulence intensity at the lower section of the pipe, where the solid volume fraction is higher due to gravity. This is in good agreement with the experimental measurements.

Comparison between the experimental and simulation results showed that for all simulations, the standard k-ε turbulence model and the k-ε turbulence model with hybrid source terms are not capable of predicting the detail of turbulence intensity in horizontal and vertical profiles, especially for the regions close to the pipe wall. However, the general trend of turbulence intensity is captured. The standard k-ε turbulence model could not predict the turbulence intensity increase in the lower section of the pipe where more particles are conveyed because there is no term in the standard k-ε turbulence model to take into account the presence of particles. It was also observed that in some cases the addition of source terms did not generally

improve the simulation results. Therefore, before initiating any simulations it may be needed to check if these source terms are required based on the operating conditions. If these source terms are applied, the $C_{\varepsilon 3}$ value needs to be calibrated. The results suggest that the k-ε turbulence model is not well suited to modelling a particle-fluid system where turbulence modulation is important, and there is thus a necessity to develop a turbulence model which can be applied for such particle laden flows. Turbulence modulation source terms including the particle-particle interaction and lift force effects may also be derived and implemented into a CFD-DEM framework as a future study.

Acknowledgment

The authors wish to thank DEM-Solutions Limited for their assistance with this work.

This work has been carried out as a part of the PARDEM project, an EU-funded, Framework 7 Marie Curie Initial Training Network. The financial support provided by the European Commission is gratefully acknowledged.

Nomenclature

C_D	Drag coefficient
e	Coefficient of restitution
G^*	Equivalent shear modulus(pa)
I_i	Particle moment of inertia(kg.m^2)
k	Turbulent kinetic energy(m^2/s^2)
m_i	Particle mass(kg)
m^*	Equivalent mass(kg)
R^*	Equivalent radius(m)
$T_{i,j}$	Torque(N.m)
u_p	Particle velocity(m/s)
u'_{pi}	Particle fluctuating velocity(m/s)
$\bar{u}_p$	Mean particle velocity(m/s)
v'_i	Gas fluctuating velocity(m/s)
$\bar{v}$	Mean gas velocity (m/s)
V_t^{rel}	Relative tangential velocity(m/s)
V_n^{rel}	Relative normal velocity(m/s)
ω_p	Particle angular velocity(rad/s)
Y^*	Equivalent Young's modulus(pa)

Greek letters

δ_n	Normal overlap(m)
δ_t	Tangential overlap(m)
ε	Dissipation (m^2/s^3)
μ	Dynamic viscosity(Pa.s)
μ_r	Coefficient of rolling friction
μ_s	Coefficient of static friction
ρ	Fluid density(kg/m^3)
ρ_p	Particle density(kg/m^3)
τ_e	Eddy turnover time(s)
τ_r	Rolling friction
τ_p	Particle response time(s)
ϕ_p	Particle volume fraction

References:

Bolio, E. J., & Sinclair, J. L. (1995). Gas turbulence modulation in the pneumatic conveying of massive particles in vertical tubes. *International Journal of Multiphase Flow, 21*, 985-1001.

Boulet, P., & Moissette, S. (2002). Influence of the particle-turbulence modulation modelling in the simulation of a non-isothermal gas-slid flow. *International Journal of Heat and Mass Transfer, 45*, 4201-4216.

Chen, C. P., & Wood, P. E. (1985). A turbulence closure model for dilute gas-particle flows. *The Canadian Journal of Chemical Engineering, 63*, 349-360.

Crowe, C. T. (2000). On models for turbulence modulation in fluid-particle flows. *International Journal of Multiphase Flow, 26*, 719-727.

Curtis, J. S., & van Wachem, B. (2004). Modeling particle-laden flows: A research outlook. *AIChE Journal, 50*, 2638-2645.

Ebrahimi, M., Crapper, M., & Ooi, J. Y. (2014). Experimental and Simulation Studies of Dilute Horizontal Pneumatic Conveying. *Particulate Science and Technology, 32*, 206-213.

Elghobashi, S. (1994). On predicting particle-laden turbulent flows. *Applied Scientific Research, 52*, 309-329.

Elgobashi, S. E., & Abou-Arab, T. W. (1983). A two-equation turbulence model for two-phase flows. *Physics of Fluids, 26*, 931-938.

Ergun, S. (1952). Fluid flow through packed columns. *Chemical Engineering Progress, 48*, 89-94.

Fan, J., Zhang, X., Cheng, L., & Cen, K. (1997). Numerical simulation and experimental study of two-phase flow in a vertical pipe. *Aerosol science and technology, 3*, 281-292

Fokeer, S., Kingman, S., Lowndes, I., & Reynolds, A. (2004). Characterisation of the cross sectional particle concentration distribution in horizontal dilute flow conveying-a review. *Chemical Engineering and Processing: Process Intensification, 43*, 677-691.

Geiss, S., Dreizler, A., Stojanovic, Z., Chrigui, M., Sadiki, A., & Janicka, J. (2004). Investigation of turbulence modification in a non-reactive two-phase flow. *Experiments in Fluids, 36*, 344-354.

Gore, R. A., & Crowe, C. T. (1989). Effect of particle size on modulating turbulent intensity. *International Journal of Multiphase Flow, 15*, 279-285.

Gouesbet, G., & Berlemont, A. (1998). Eulerian and Lagrangian approaches for predicting the behaviour of discrete particles in turbulent flows. *Progress in Energy and Combustion Science, 25*, 133-159.

Henthorn, K. H., Park, K., & Curtis, J. S. (2005). Measurement and prediction of pressure drop in pneumatic conveying: Effect of particle characteristics, mass loading, and Reynolds number. *Industrial & Engineering Chemistry Research, 44*, 5090-5098.

Hetsroni, G. (1989). Particles-turbulence interaction. *International Journal of Multiphase Flow, 15*, 735-746.

Hwanc, G. J., & Shen, H. H. (1993). Fluctuation energy equations for turbulent fluid-solid flows. *International Journal of Multiphase Flow, 19*, 887-895.

Kenning, V. M., & Crowe, C. T. (1997). On the effect of particles on carrier phase turbulence in gas-particle flows. *International Journal of Multiphase Flow, 23*, 403-408.

Kulick, J., Fessler, J., & Eaton, J. (1994). Particle response and turbulent modification in fully-developed channel flow. *JOURNAL OF FLUID MECHANICS, 277*, 109-134.

Laín, S., Bröder, D., Sommerfeld, M., & Göz, M. (2002). Modelling hydrodynamics and turbulence in a bubble column using the Euler–Lagrange procedure. *International Journal of Multiphase Flow, 28*, 1381-1407.

Laín, S., & Sommerfeld, M. (2003). Turbulence modulation in dispersed two-phase flow laden with solids from a Lagrangian perspective. *International Journal of Heat and Fluid Flow, 24*, 616-625.

Laín, S., & Sommerfeld, M. (2008). Euler/Lagrange computations of pneumatic conveying in a horizontal chanel with different wall roughness. *Powder Technology, 184*, 76-88.

Lightstone, M. F., & Hodgson, S. M. (2004). Turbulence Modulation in Gas-Particle Flows: A Comparison of Selected Models. *The Canadian Journal of Chemical Engineering, 82*, 209-219.

Lu, Y., Glass, D., Easson, W. J., & Crapper, M. (2008). Investigation of Flow Patterns of Gas-Solid Granular Flow over Horizontal Pipe Cross-sections by FLUENT & EDEM. In *Particulate Systems Analysis* Stratford-upon-Avon, United Kingdom.

Lu, Y., Glass, D. H., & Easson, W. J. (2009). An investigation of particle behaviour in gas–solid horizontal pipe flow by an extended LDA technique. *Fuel, 88*.

Lun, C. K. K. (2000). Numerical simulation of dilute turbulent gas-solid flows. *International Journal of Multiphase Flow, 26*, 1707-1736.

Mandø, M. (2009). Turbulence modulation by non-spherical particles. *Department of energy technology, Aalborg University*.

Mathisen, A., Halvorsen, B., & Melaaen, M. C. (2008). Experimental studies of dilute vertical pneumatic transport. *Particulate science and technology 26*, 235-246.

Mindlin, R. D., & Deresiewicz, H. (1953). Elastic spheres in contact under varying oblique forces. *Journal of applied mechanics, 21*, 327-344.

Oesterlé, B., & Dinh, T. B. (1998). Experiments on the lift of a spinning sphere in a range of intermediate Reynolds numbers. *Experiments in Fluids, 25*, 16-22.

Pakhomov, M. A., Protasov, M. V., Terekhov, V. I., & Varaksin, A. Y. (2007). Experimental and numerical investigation of downward gas-dispersed turbulent pipe flow. *International Journal of Heat and Mass Transfer, 50*, 2107-2116.

Rao, A., Curtis, J. S., Hancock, B. C., & Wassgren, C. (2012). Numerical simulation of dilute turbulent gas-particle flow with turbulence modulation. *AIChE Journal, 58*, 1381-1396.

Tsuji, Y., & Morikawa, Y. (1982). LDV measurements of an air-solid two-phase flow in a horizontal pipe. *Journal of Fluid Mechanics, 120*, 385-409.

Tsuji, Y., Morikawa, Y., & Shimoni, H. (1984). LDV measurements of an air-solid two-phase flow in a vertical pipe. *JOURNAL OF FLUID MECHANICS, 139*, 417-434.

Vreman, A. W. (2007). Turbulence characteristics of particle-laden pipe flow. *JOURNAL OF FLUID MECHANICS, 584*, 235-279.

Wen, C. Y., & Yu, Y. H. (1966). Mechanics of fluidisation. *Chemical Engineering Progress Symposium Series, 62*, 100-111.

Yarin, L. P., & Hetsroni, G. (1994). Turbulence intensity in dilute two-phase flows- 3 The particles-turbulence interaction in dilute two-phase flow. *International Journal of Multiphase Flow, 20*, 27-44.

Yuan, Z., & Michaelides, E. E. (1992). Turbulence modulation in particulate flows- A theoritical approach. *Int J. Multiphase Flow, 18*, 779-785.

Zhang, Y., & Reese, J. M. (2003). Gas turbulence modulation in a two-fluid model for gas–solid flows. *AIChE journal, 49*, 3048-3065.

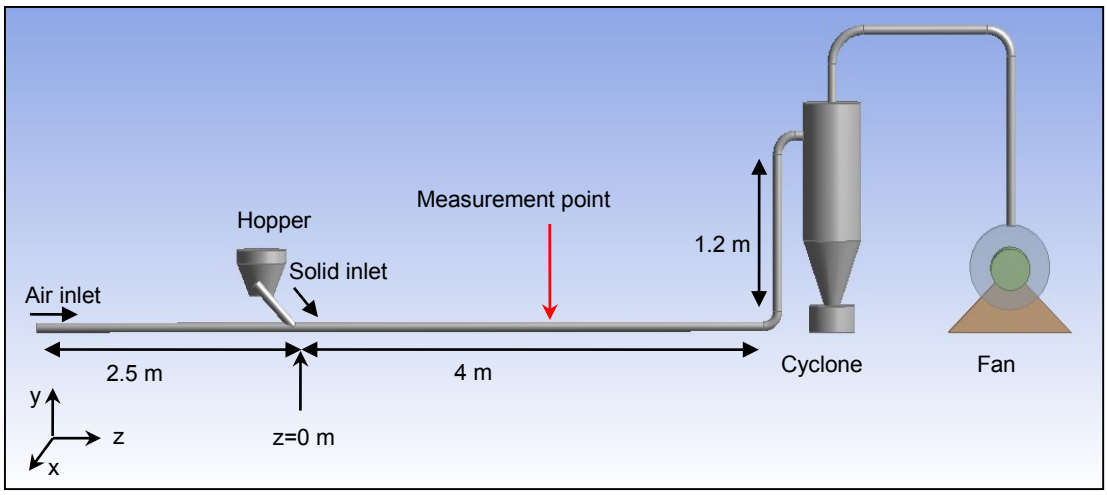

Figure 1: Schematic of pneumatic conveying system.

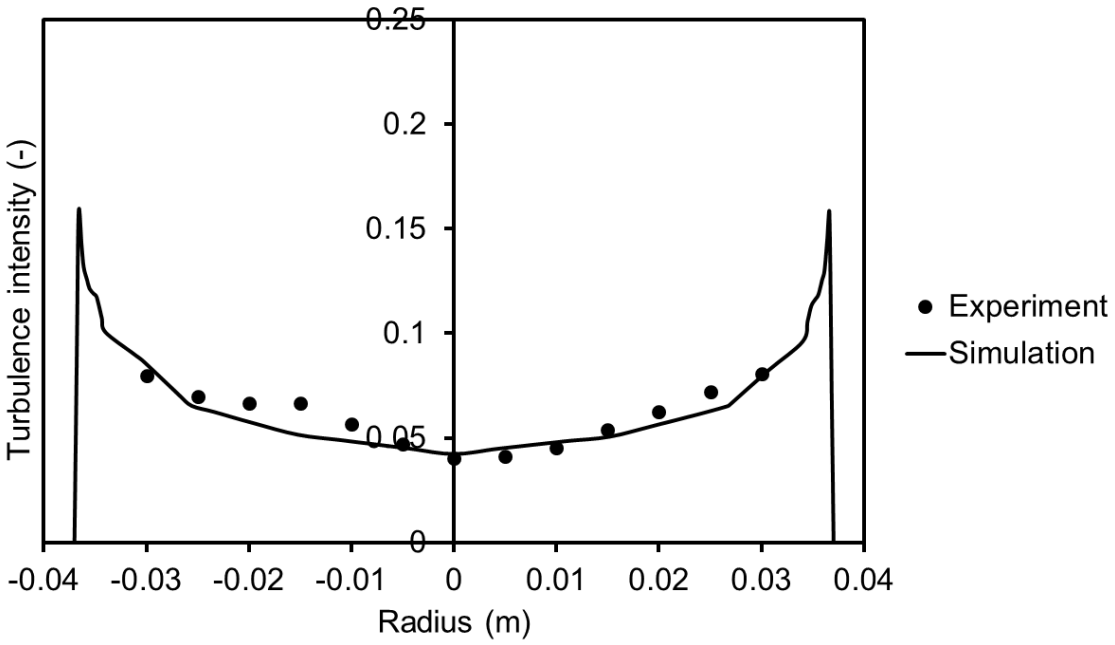

Figure 2: Horizontal profile of gas turbulence intensity for pure gas flow, gas velocity 9.5m/s.

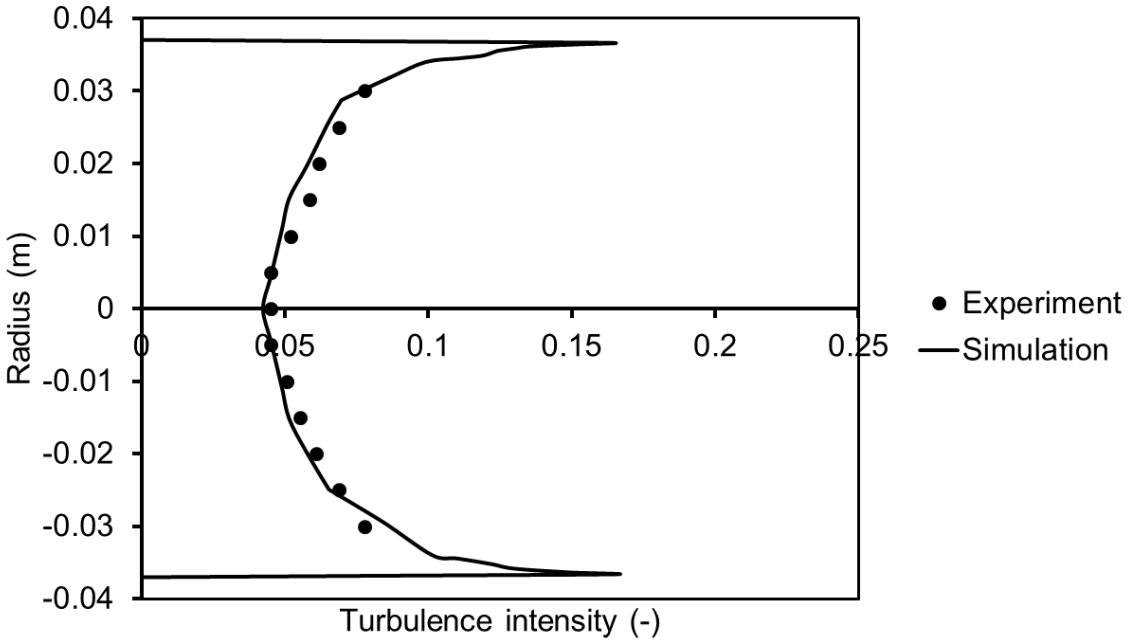

Figure 3: Vertical profile of gas turbulence intensity for pure gas flow, gas velocity 8.5m/s.

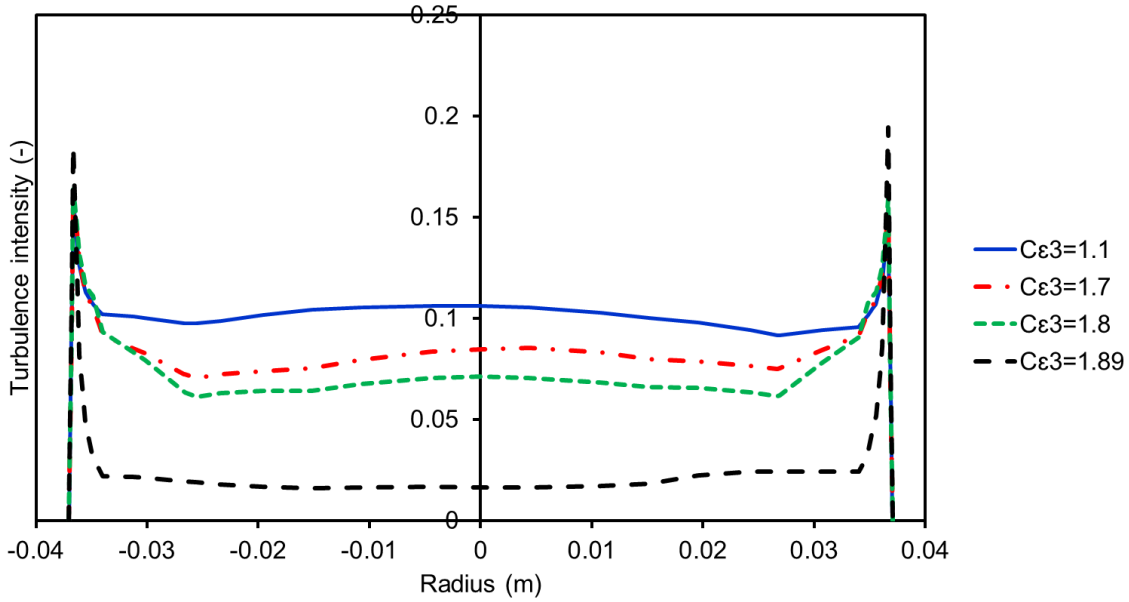

Figure 4: Effect of $C_{\varepsilon 3}$ on the horizontal profile of turbulence intensity, 2 mm particles, SLR=2.3 at z=2 m.

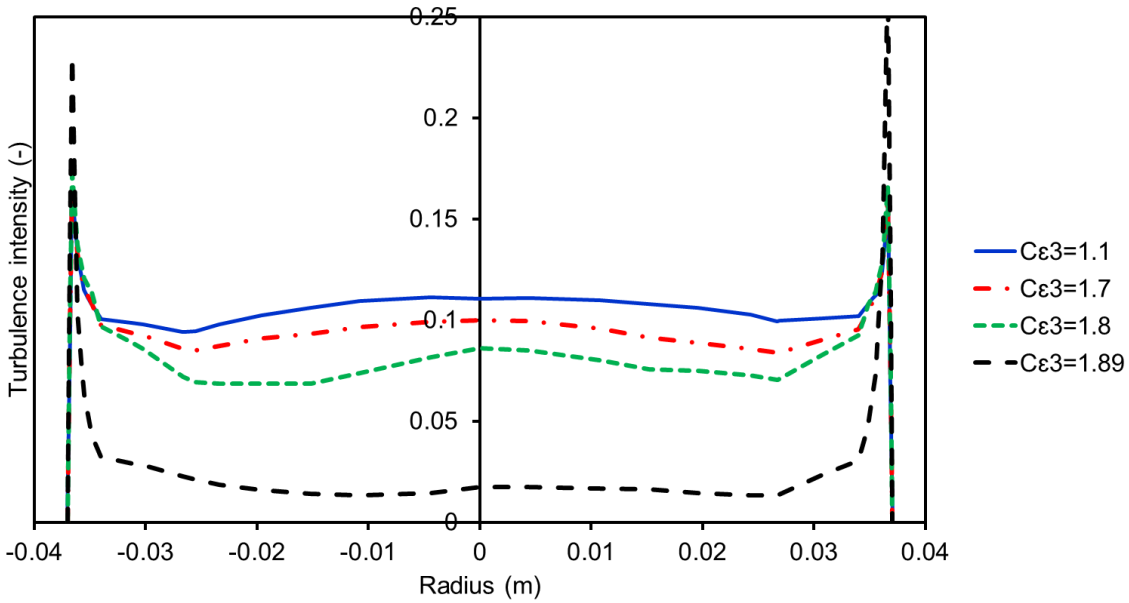

Figure 5: Effect of $C_{\varepsilon 3}$ on the horizontal profile of turbulence intensity, 2 mm particles, SLR=3 at z=2 m

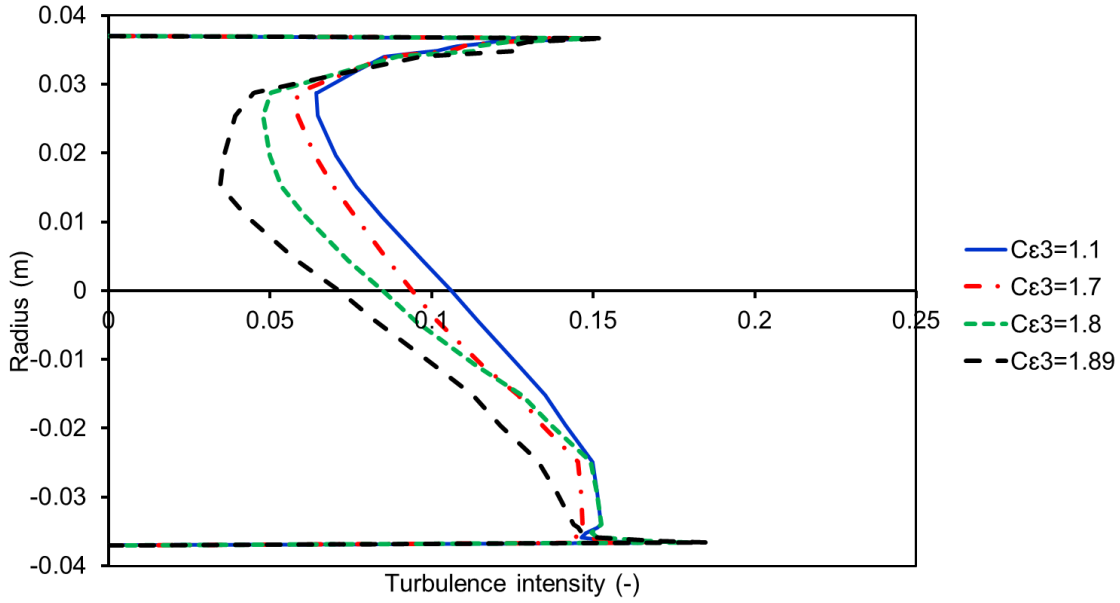

Figure 6: Effect of $C_{\varepsilon 3}$ on the vertical profile of turbulence intensity, 2 mm particles, SLR=2.3 at z=2 m.

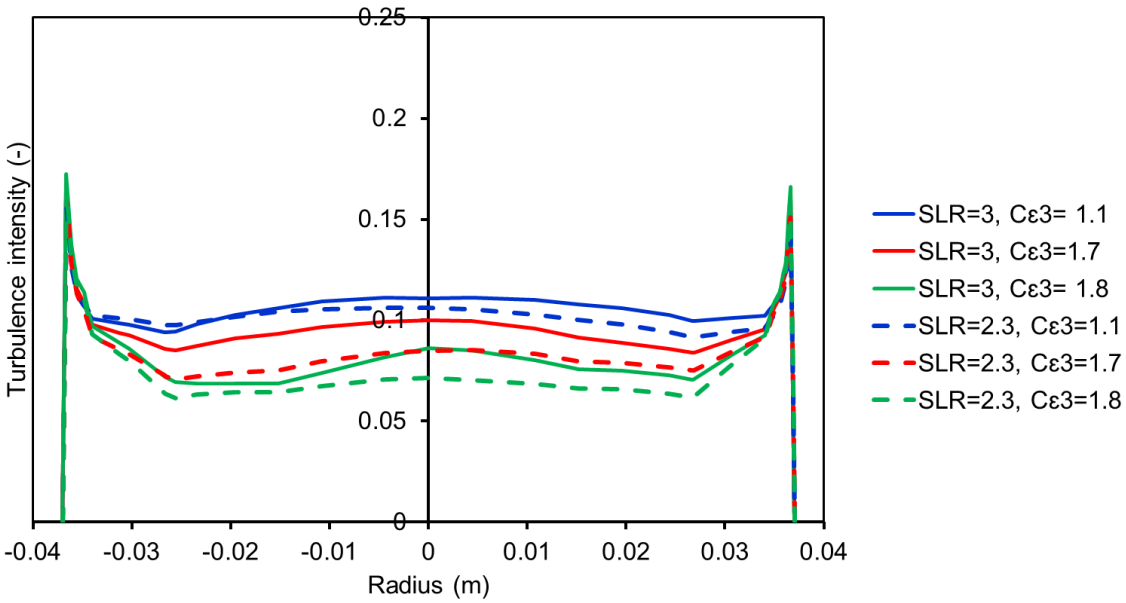

Figure 7: Influence of SLR on the turbulence intensity, 2 mm glass beads at z=2 m

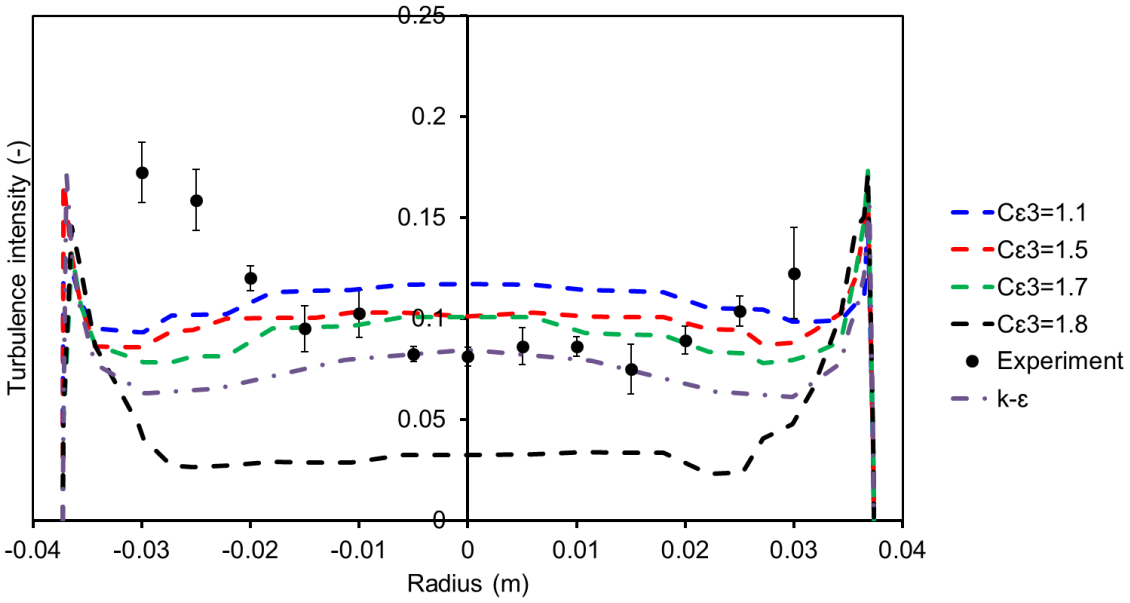

Figure 8: Effect of $C_{\varepsilon 3}$ on the horizontal profile of turbulence intensity and comparison between simulation and experimental results, 1.5 mm particles, SLR= 3 at z=2 m

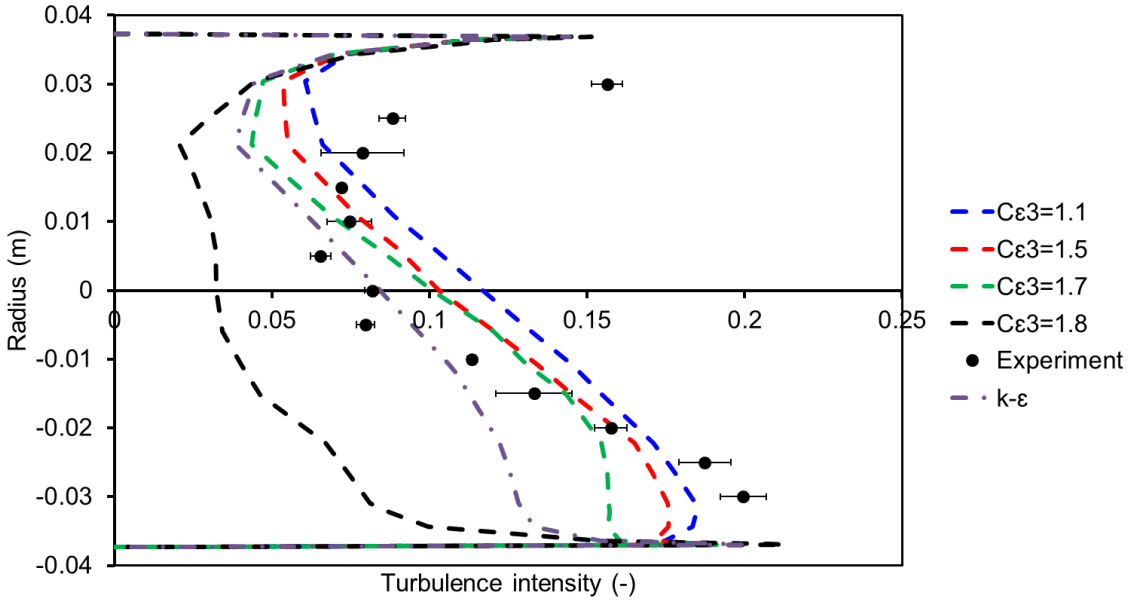

Figure 9: Effect of $C_{\varepsilon 3}$ on the vertical profile of turbulence intensity and comparison between simulation and experimental results, 1.5 mm particles, SLR= 3 at z=2 m

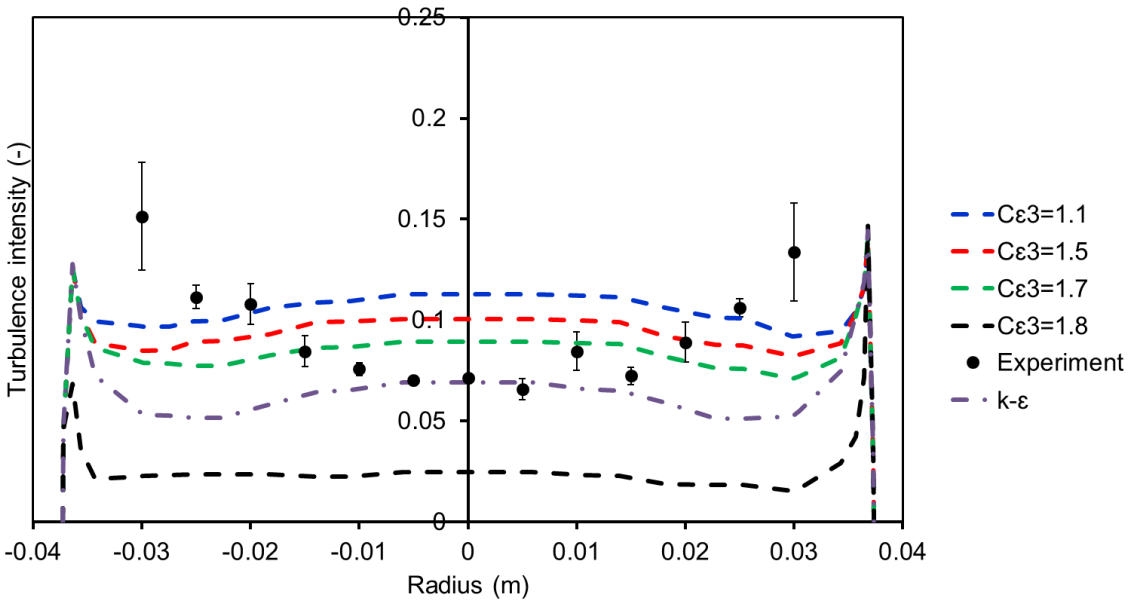

Figure 10: Effect of $C_{\varepsilon 3}$ on the horizontal profile of turbulence intensity and comparison between simulation and experimental results, 1.5 mm particles, SLR= 2.3 at z=2 m.

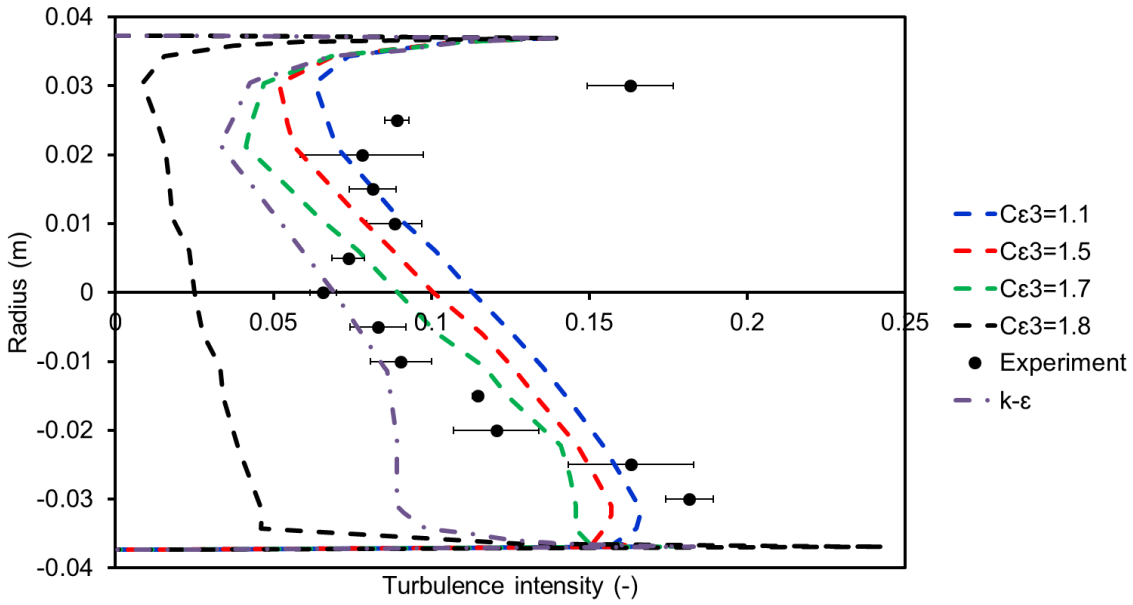

Figure 11: Effect of $C_{\varepsilon 3}$ on the vertical profile of turbulence intensity and comparison between simulation and experimental results, 1.5 mm particles, SLR= 2.3, at z=2 m

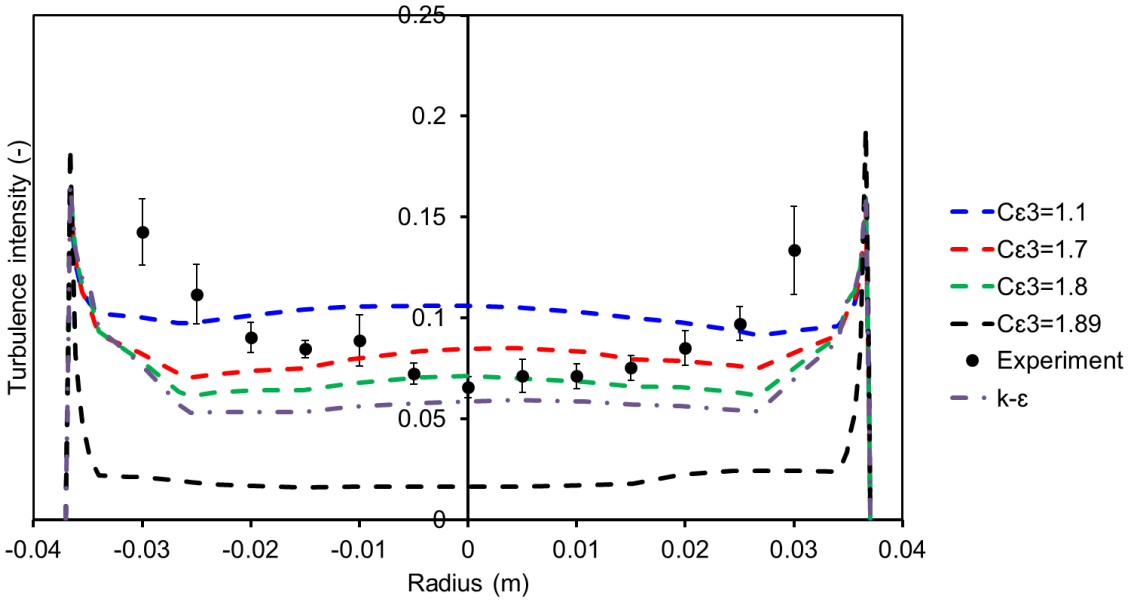

Figure 12: Effect of $C_{\varepsilon 3}$ on the horizontal profile of turbulence intensity and comparison between simulation and experimental results, 2 mm particles, SLR= 2.3, at z=2 m.

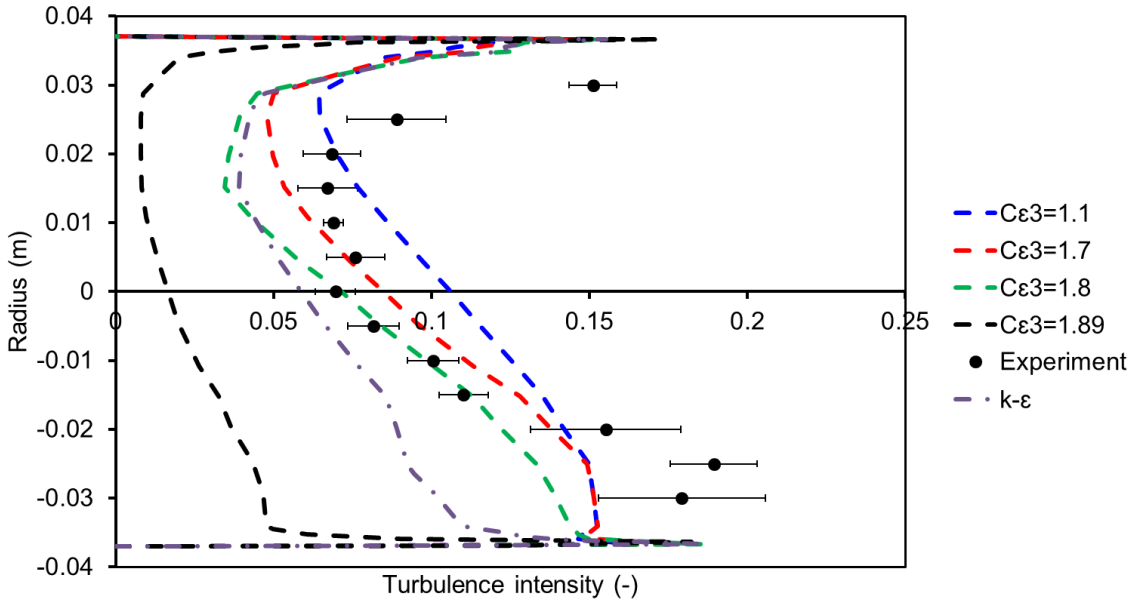

Figure 13: Effect of $C_{\varepsilon 3}$ on the vertical profile of turbulence intensity and comparison between simulation and experimental results, 2 mm particles, SLR= 2.3, at z=2 m.

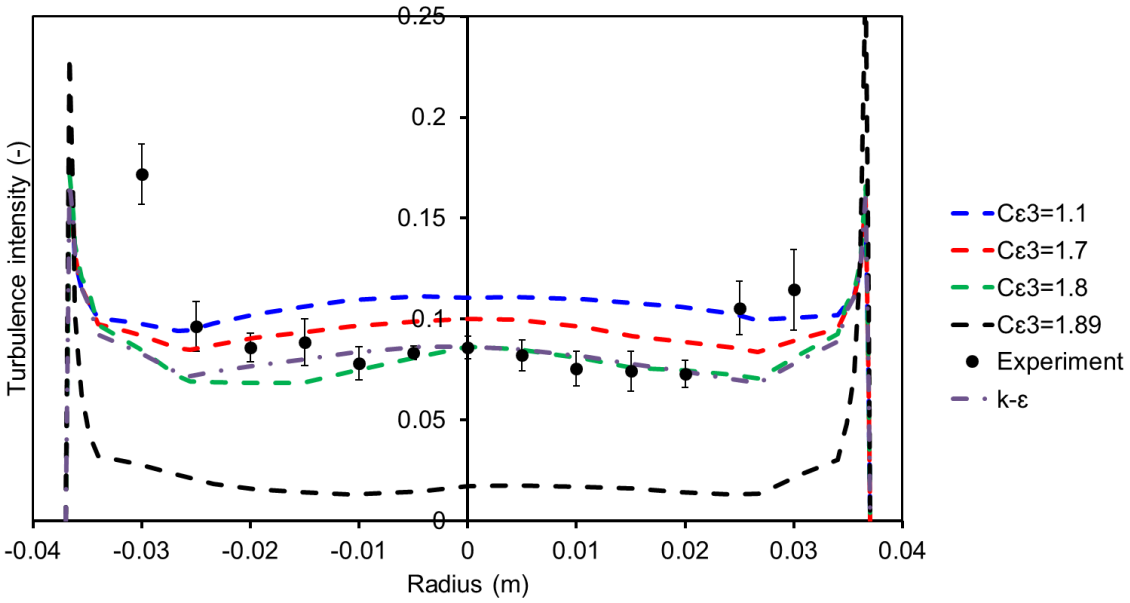

Figure 14: Effect of $C_{\varepsilon 3}$ on the horizontal profile of turbulence intensity and comparison between simulation and experimental results, 2 mm particles, SLR= 3 at z=2 m.

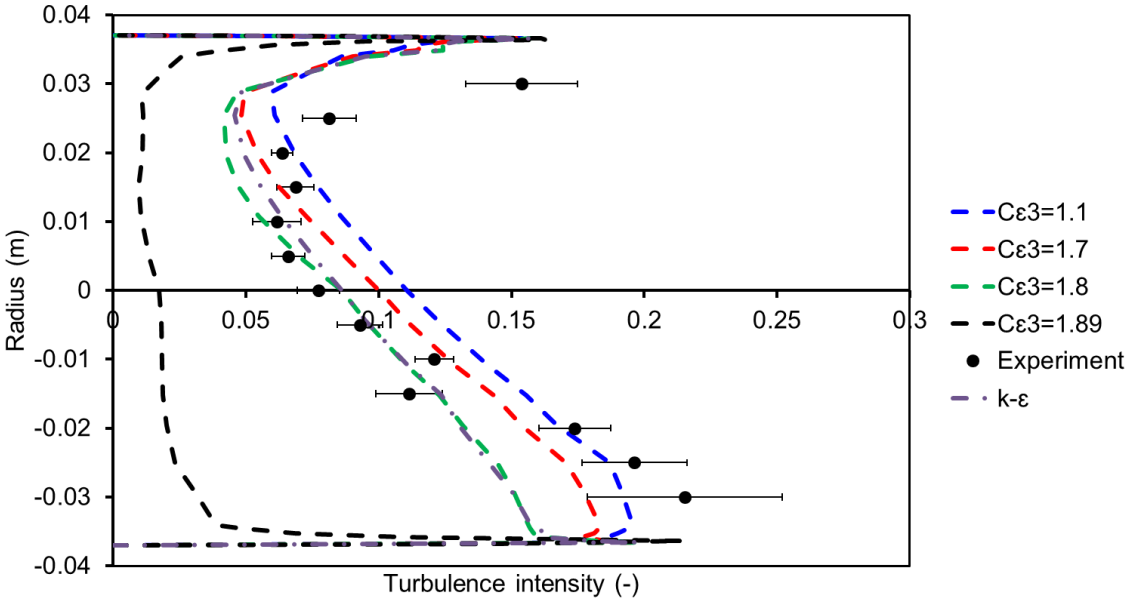

Figure 15: Effect of $C_{\varepsilon 3}$ on the vertical profile of turbulence intensity and comparison between simulation and experimental results, 2 mm particles, SLR= 3 at z=2 m.

Table 1: Numerical parameters for FLUENT-EDEM simulation

Simulation method	CFD-DEM (Eulerian-Lagrangian)
Coupling method	Two-way coupling
FLUENT	
Air density (kg/m^3)	1.225
Air viscosity (pa.s)	1.78e-5
Wall boundary	No-slip condition
Turbulence model	Standard k-ε model or k-ε model with the hybrid source terms
EDEM	
Particle creation	Created in the inclined pipe with the initial velocity similar to the experiments
Particle flow rate (kg/s)	0.1128, 0.1329
Poisson's ratio	0.24
Shear modulus(pa)	2.62e10
Particle-Particle, Particle-wall contact model	Non-linear Hertz-Mindlin
Particle diameter (m)	0.0015, 0.002
Particle density (kg/m^3)	2540
Coefficient of restitution (glass beads-wall)	0.97
Coefficient of restitution (glass beads-glass beads)	0.9
Coefficient of static friction	0.154
Coefficient of rolling friction	0.1
Time step	3.0e-7
Gas-Particle interactions	
Drag model	Ergun and Wen&Yu
Lift model	Magnus lift force